·Proc. XXXIst Rencontres de Moriond
Les Arcs, Savoie, France
March 23-30, 1996

BNL-64198

DISTRIBUTION OF THIS DOCUMENT IS UNLIMITED

CONF-9603173--22

THE PHYSICS AND DETECTORS OF THE RELATIVISTIC HEAVY ION COLLIDER (RHIC)*

RECEIVED
APR 07 1997
OSTI

T. J. Hallman
Brookhaven National Laboratory, Upton, New York, 11973, U.S.A.

1. INTRODUCTION

In mid-1999 the Relativistic Heavy Ion Collider (RHIC) facility at Brookhaven National Laboratory will begin accelerating ^{197}Au nuclei to 100 A GeV. The effective temperature in the dense region of overlap when two nuclei collide nearly head on at this energy is expected to reach $\sim 10^{12}$ degrees Kelvin. At this temperature a basic restructuring of matter is expected to occur, in which the quark and gluon constituents normally confined in hadronic matter form a chirally symmetric deconfined plasma.

Experience at lower energies (Bevalac, AGS, SPS) has provided many exciting results, the interpretation of which is nevertheless difficult in terms of isolating fundamentally new physics. The RHIC physics program has been crafted to answer definitively the question of the existence of a deconfinement transition at $\sqrt{s_{nn}} = 200$ GeV by taking adavantage of two aspects that are fundamentally new in this regime: correlations of global observables and hard scattering of partons.

There are many signatures which have been proposed to help isolate evidence of a transition to a deconfined phase of matter[1]. These include, for example:

- strangeness "saturation" on a time scale (10fm/c) too short to be accounted for by strangeness exchange interactions in a hadron gas
- color screening (vector meson suppression) in the plasma phase
- in-medium effects on the mass/lifetime of the vector mesons
- the observation of thermodynamic/chemical equilibrium
- thermal radiation from a hot plasma
- "excess" heavy flavor (e.g. open charm) production
- a discontinuity or change in the correlation between energy density and entropy density
- the observation of a long hadronization time
- dioriented chiral condensate behavior (isospin or low p_t correlations)

MASTER

Each of the RHIC detectors is optimized for the measurement of a number of the above signatures. It is therefore possible because of the very high particle densities at RHIC ($dn/d\eta \approx 1000$) for these detectors to correlate multiple observables in a single event or in a sample of events which has been selected as "interesting" on the basis of the observation of one or more plasma signatures. In this way it will be possible to isolate events which exhibit correlated non-statistical fluctuations in several observables simultaneously.

It will also be possible at RHIC to make a self-consistent measurement of the "initial conditions", and in particular the gluon distribution in the nucleus. This will afford optimal use of perturbative QCD in providing guidance as to the evolution of the early stages of the collision.

The following sections contain a brief review of the design and capabilities of the four detectors at RHIC. Due to space limitations, a discussion of the exciting spin physics program at RHIC will be deferred.

*This research was supported by the U.S. Department of Energy under contract Nos. DE-AC02-76CH00016.

1.1. The Broad RAnge Hadron Magnetic Spectrometers (BRAHMS)

The Broad RAnge Hadron Magnetic Spectrometers (BRAHMS) experiment (Fig. 1) includes two small solid angle spectrometers which cover the angular region from 2° to 20° and 20° to 90° respectively, as well as a midrapidity spectrometer. In the forward spectrometer, tracking is provided both by TPC modules (T1, T2, T3) and conventional drift chambers (T4, T5). Two TOF hodoscopes (H1, H2) in this arm allow for π/K separation (4σ) up to 3.3 and 5 GeV/c respectively. The corresponding ranges for K/p separation are 5.7 and 8.5 GeV/c. The tracking chambers are located in a complex of 4 magnets (D1–D4), allowing for separate coverage from 2.5–6 GeV/c (D1-D2) and 4–25 GeV/c (D1–D4). A segmented threshold gas Čerenkov counter provides further PID at a location behind D2, while a ring imaging Čerenkov counter behind D4 allows for K/π and K/p separation up to 25 GeV/c.

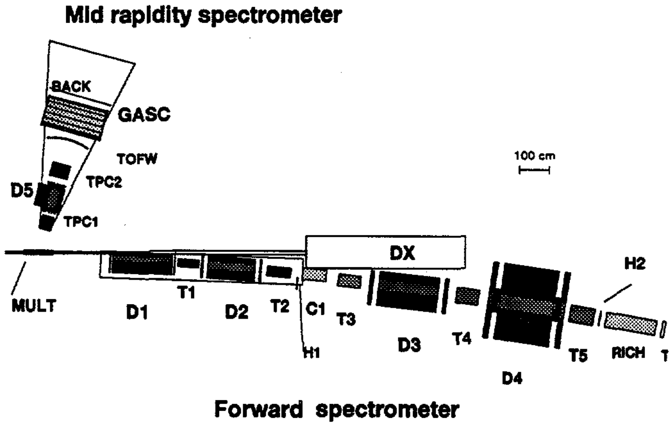

Figure 1. Detector layout for the BRAHMS spectrometers.

One important aspect of the BRAHMS physics program will be inclusive and semi-exclusive measurements of the particle yields ($\pi^{\pm}$, $K^{\pm}$, $p^{\pm}$) as a function of rapidity and p_t. There is presently a large discrepancy between various models as to the degree of stopping at RHIC and the corresponding rapidity density for the net baryon number in the "baryon free" region for central AuAu collisions. The large acceptance in y ($|y| \leq 4$) and p_t (≤ 2.5 GeV/c) of the BRAHMS spectrometer complex affords the means for a key element of the proposed physics program – to establish constraints on theoretical models in order to understand the basic physical processes for heavy ion collisions at RHIC.

1.2. PHENIX

The PHENIX detector (Fig. 2) is a high rate capability detector designed to be capable of simultaneous investigation of a number of signatures of the Quark Gluon Plasma (QGP) at RHIC. The physics topics to be explored include deconfinement and color screening, chiral symmetry restoration, thermal radiation of a hot gas, strangeness and charm production, space time evolution of the plasma, and other topics. The experimental plan is to measure leptons (electrons and muons), photons, and hadrons as a function of the energy density in heavy ion collisions. The detector will have three spectrometers; the Central Magnet (CM), the Muon Magnet (MM North), and the South Muon Magnet which will be added as an upgrade.

The CM spectrometer covers an interval of ± 0.35 units in rapidity and 180° in ϕ. The ϕ coverage is split into two 90° arms separated by 67.5°.

The di-electron invariant mass spectrum resulting from a full simulation of the PHENIX electron ID capabilities is shown in Fig. 3. The PHENIX tracking and RICH detectors which allow for electron-hadron separation at the level of $> 10^{-4}$ from a few hundred MeV to about

DISCLAIMER

This report was prepared as an account of work sponsored by an agency of the United States Government. Neither the United States Government nor any agency thereof, nor any of their employees, make any warranty, express or implied, or assumes any legal liability or responsibility for the accuracy, completeness, or usefulness of any information, apparatus, product, or process disclosed, or represents that its use would not infringe privately owned rights. Reference herein to any specific commercial product, process, or service by trade name, trademark, manufacturer, or otherwise does not necessarily constitute or imply its endorsement, recommendation, or favoring by the United States Government or any agency thereof. The views and opinions of authors expressed herein do not necessarily state or reflect those of the United States Government or any agency thereof.

DISCLAIMER

Portions of this document may be illegible in electronic image products. Images are produced from the best available original document.

4 GeV, while the TEC has good dE/dx sampling below 2 GeV and electron-hadron separation at the level of 10^{-2}. A further e/π discrimination of $\approx 10^{-2}$ is accomplished using the TOF capabilities of the Pb-Scintillator electromagnetic calorimeter (TOF resolution is $\approx 70\ ps/\sqrt{E} + 70\ ps$) which is effective for particle energies $\lesssim 1$ GeV.

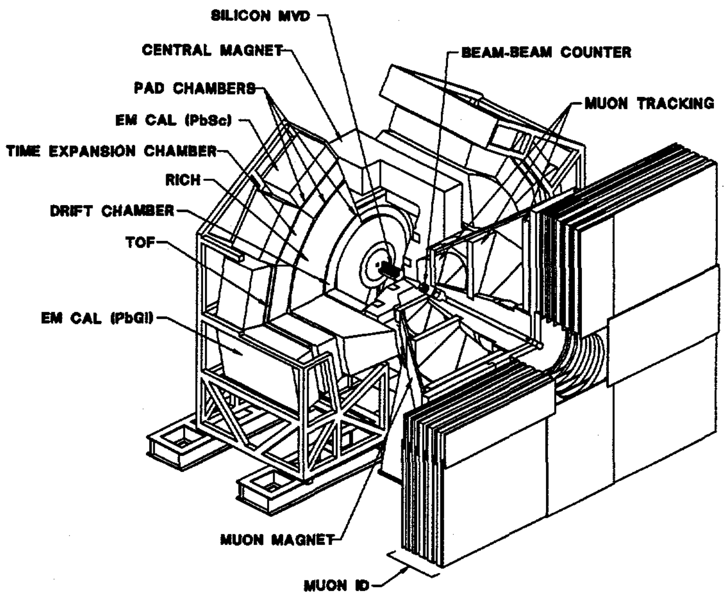

Figure 2. Schematic layout of the PHENIX detector.

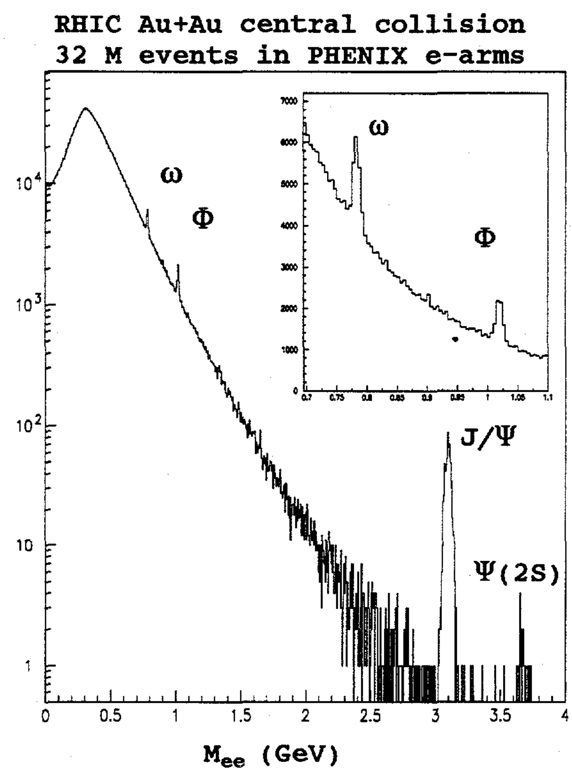

Figure 3. The di-electron invariant mass spectrum for 1 week of RHIC running from a simulation of the PHENIX electron detection capability.

The PHENIX EMCAL sections will also be used for the measurement of direct photons and π^0 spectra, and to search for anomalous fluctuations in the ratio of neutral to charged mesons.

At a temperature of about 500 MeV, as might be expected from a "hot glue scenario"[2], the PHENIX EM calorimeter is sensitive to the direct photon signal for $p_t \gtrsim 1$ GeV/c using the lead glass and *Pb*-scintillator sections.

In addition to studying color screening through J/ψ suppression studies in the di-electron channel, PHENIX will also study J/ψ production by reconstructing di-muon pairs. This will be accomplished using the MM muon spectrometer arm. Simulation of the dimuon event rate into PHENIX in a canonical RHIC year was noted to result in the following yields:

Table 2

	Central *AuAu*	Min. Bias *AuAu*	Min. Bias *pAu*
$\phi \to \mu^+\mu^-$	58,000	210,000	176,000
$J/\psi \to \mu^+\mu^-$	249,000	1,107,000	678,000
$\psi' \to \mu^+\mu^-$	3,650	15,490	9,400
$\Upsilon \to \mu^+\mu^-$	932	3,890	1,100
$\Upsilon' \to \mu^+\mu^-$	95	400	110

The signal to noise ratio at the ϕ resonance is 1:100; at the J/ψ is is 3:1, and at the Υ, 300:1.

1.3. PHOBOS

A schematic view of the PHOBOS detector is shown in Fig. 4. The PHOBOS detector is designed to detect as many of the particles produced in 200 A GeV *AuAu* interactions at RHIC as possible. This will be accomplished at high pseudorapidity ($|\eta| \leq 5.4$) using annular arrays of silicon pad detectors. To determine the yield of final state photons, thin radiators will be installed in front of alternate silicon pads. For particles having $|\eta| \leq 3$, particles will be detected by silicon strips.

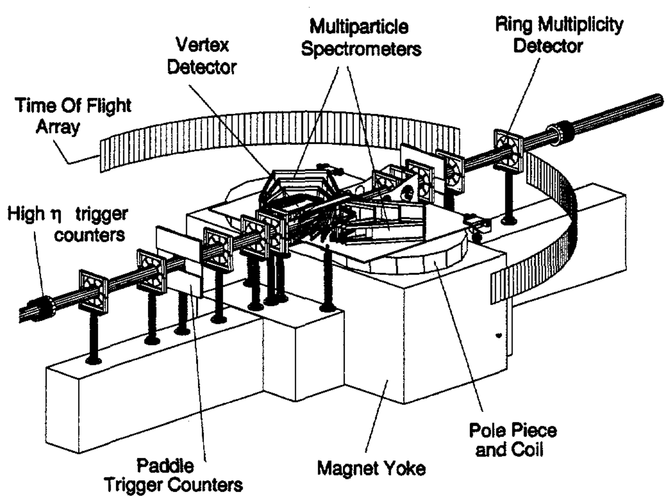

Figure 4. A schematic view of The PHOBOS detector.

For approximately 1% of the produced particles, detailed information (momentum, PID) will be provided by a two-arm multi-particle spectrometer ($0.5 < \eta < 1.5$) located on either side of the interaction volume and displaced to one side of the interaction diamond so that particles having transverse momenta as low as 30 MeV/c can enter the magnetic volume. Tracking in the spectrometer arms is accomplished by 6 layers of silicon pads followed by 6 layers of silicon strips. Particle identification for particles in this acceptance is accomplished by ionization energy loss in the $1/\beta^2$ region.

The large acceptance planned for the PHOBOS experiment allows for a sensitive search for fluctuations possibly indicative of new physics. It is noted for example that fluctuations of 5–10% in the particle production over one unit of pseudorapidity would be quite apparent in the measured $dn/d\eta$ distributions. Such a fluctuation might result in the hadronization of a QGP, if local excitation of the QCD vacuum within the collision volume resulted, prior to hadronization, in two vacua being in proximity with different spontaneously broken symmetry states[3].

1.4. The Solenoidal Tracker at RHIC (STAR)

The Solenoidal Tracker At RHIC (STAR) (Fig. 5) is designed to search for signatures of QGP formation through the measurement and correlation of global observables on an event-by-event basis and the use of hard scattering of partons to probe the properties of high density matter. The STAR detector utilizes a time projection chamber (TPC) in a solenoidal magnetic field of 0.5T covering approximately 4 units of the central rapidity. Additional elements of the detector include a silicon vertex tracker (SVT) to locate the position of the primary vertex and to locate secondary vertices to an accuracy of 20 μm. A Pb-scintillator sampling electromagnetic calorimeter will be used to trigger on transverse energy and measure jets, direct photons and leading π^0 production. A portion of the acceptance will be instrumented with a highly segmented TOF array, extending the maximum momentum for π/K separation from 0.6 to 1.5 GeV/c and the corresponding limit for K/p separation from 1–2.4 GeV/c. External TPCs (XTPC) located in the forward regions will be used to study the transfer of energy from projectile rapidity to midrapidity by following the fate of the incident baryons rescattered in the collision.

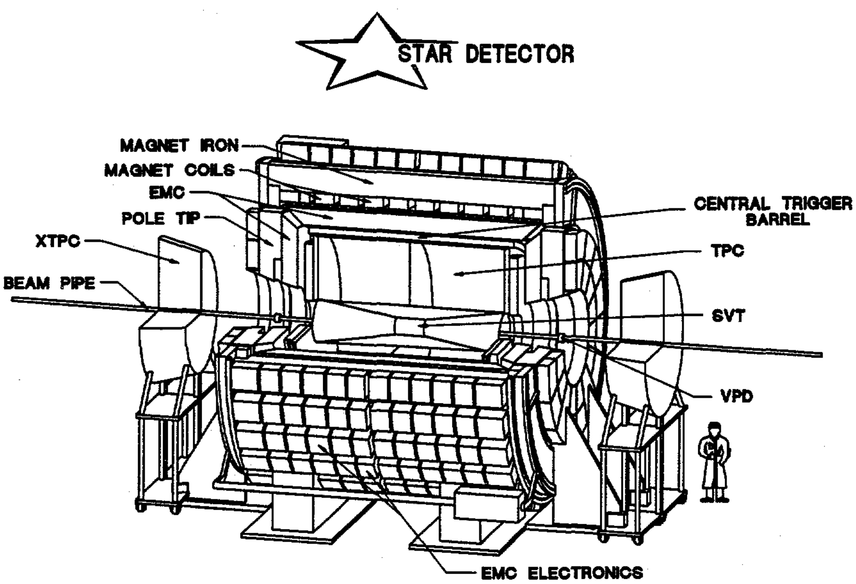

Figure 5. Schematic layout of the STAR detector.

One important aspect of the STAR program will be to search for special events in which the measurement and correlation of event-by-event observables (e.g. dn_π/dy, T_π, K/π, $p_{t\pi}$, dn/dy) indicates the transition to a deconfined phase may have occurred. A second goal will be to measure the thermodynamic observables (T, μ_B, μ_s) for an ensemble of events to establish whether a state of thermal and chemical equilibrium has been reached. The design of the detector allows for the precise measurement, for example, of particle ratios ($p/\bar{p}$, $\bar{\Lambda}/\Lambda$, K/π) to determine the strange chemical and baryo-chemical potentials, inverse slope parameters and p_t

to determine the energy density (temperature), and dn/dy distributions to investigate entropy production.

Determination of the strangeness density in relativistic heavy ion collisions and strangeness saturation have long been recognized[4] as important probes of plasma production. In STAR the identification of secondary vertices from strange particle decays is accomplished with a new type of detector developed at Brookhaven National Laboratory (BNL) through RHIC R&D – the silicon drift detector (SDD). Using the characteristic resolutions demonstrated through R&D for this device, the Ξ yield expected for $AuAu$ running is shown in Fig. 6.

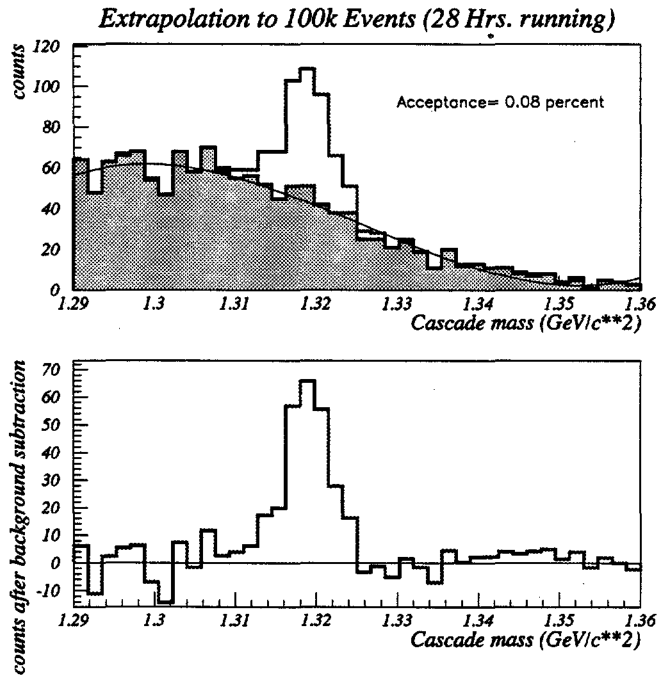

Figure 6. Simulated invariant mass distribution for the Ξ using the STAR SVT.

Another important element in the ion studies at RHIC and LHC will be the determination of the initial conditions – the gluon distribution in the nucleus[5]. In STAR a program of using jet + direct photon coincidences will be used to to make a direct measurement of the gluon distribution in pAu interactions.

2. CONCLUSIONS

The design of the collider detectors for RHIC is well matched to the physics goals of searching for a new deconfined phase of matter. The physics of different detectors at RHIC is complimentary, providing for a well balanced program.

REFERENCES

1. J.W. Harris, B. Muller, The Search for the Quark-Gluon Plasma, (to be published).
2. E. V. Shuryak, Phys. Lett. 78B (1978) 150; M. T. Strickland, Phys. Lett. B331 (1994) 245; D. K. Stivastava, B. Sinha, M. Gyulassy, and X. N. Wang, Phys. Lett. B276 (1992) 285.
3. See, for example, S. Gavin, Nuc. Phys. A590 (1995) 163c.
4. J. Rafelski, Phys. Lett. B262 (1991) 333; see also E. Andersen et al., Phys. Lett. B327 (1994) 433, and references therein.
5. K. J. Eskola, Jianwei Qiu, and Xin-Nian Wang, Phys. Rev. Lett. 72 (1994) 36.